Scientific Reports

https://doi.org/10.1038/s41598-026-38701-6

Article in Press

Physcion-8-O-β-D-monoglucoside protects hepatocytes from TNF-α-mediated apoptosis by suppressing the PI3K/AKT/NF-κB signaling pathway

Received: 5 September 2025

Accepted: 30 January 2026

Published online: 09 March 2026

Cite this article as: Hu R., Chen Z., Chen T. *et al.* Physcion-8-O-β-D-monoglucoside protects hepatocytes from TNF-α-mediated apoptosis by suppressing the PI3K/AKT/NF-κB signaling pathway. *Sci Rep* (2026). https://doi.org/10.1038/s41598-026-38701-6

Ruoying Hu, Zhihui Chen, Ting Chen, Zixin Chen, Wenchuan Luo, Wen Xu, Mei Huang, Lihong Nan, Ru Jia, Yuqin Zhang & Yaping Chen

We are providing an unedited version of this manuscript to give early access to its findings. Before final publication, the manuscript will undergo further editing. Please note there may be errors present which affect the content, and all legal disclaimers apply.

If this paper is publishing under a Transparent Peer Review model then Peer Review reports will publish with the final article.

ARTICLE IN PRESS

© The Author(s) 2026. **Open Access** This article is licensed under a Creative Commons Attribution-NonCommercial-NoDerivatives 4.0 International License, which permits any non-commercial use, sharing, distribution and reproduction in any medium or format, as long as you give appropriate credit to the original author(s) and the source, provide a link to the Creative Commons licence, and indicate if you modified the licensed material. You do not have permission under this licence to share adapted material derived from this article or parts of it. The images or other third party material in this article are included in the article's Creative Commons licence, unless indicated otherwise in a credit line to the material. If material is not included in the article's Creative Commons licence and your intended use is not permitted by statutory regulation or exceeds the permitted use, you will need to obtain permission directly from the copyright holder. To view a copy of this licence, visit http://creativecommons.org/licenses/by-nc-nd/4.0/.

ARTICLE IN PRESS

Physcion-8-O-β-D-monoglucoside protects hepatocytes from TNF-α-mediated apoptosis by suppressing the PI3K/AKT /NF-κB signaling pathway

Ruoying Hu[1,*], Zhihui Chen[1,*], Ting Chen[2,*], Zixin Chen[1], Wenchuan Luo[1], Wen Xu[1], Mei Huang[1], Lihong Nan[1✉], Ru Jia[1✉], Yuqin Zhang[1✉], Yaping Chen[1✉]

[*]These authors contributed equally to this work.

[1] College of Pharmacy, Fujian University of Traditional Chinese Medicine, Fuzhou, Fujian 350122, China;

[2] Department of Pharmacy, Anyuan County People's Hospital, GanZhou, JiangXi, 342100, China

✉email:

Lihong Nan, 2002017@fjtcm.edu.cn; Ru Jia, 1996031@fjtcm.edu.cn; Yuqin Zhang, 2016003@fjtcm.edu.cn; Yaping Chen, 2018038@fjtcm.edu.cn.

ARTICLE IN PRESS

Abstract

Physcion-8-O-β-D-monoglucoside (PMG) is one of the active ingredients of Radix et Rhizoma Rhei, which has been used for treating liver disorders for hundreds of years in China. However, the hepatoprotective effects of PMG remain poorly understood. This study aimed to investigate the mechanism of the protection effects

ARTICLE IN PRESS

of PMG on Tumor necrosis factor-α (TNF-α)-induced hepatotoxicity. We developed both *in vitro* and *in vivo* models of liver injury to assess the protective effects of PMG against TNF-α-induced hepatotoxicity. The *in vitro* model employed TNF-α/actinomycin D in AML-12 cells, while the *in vivo* model utilized intraperitoneal injection of carbon tetrachloride (CCl_4) in mice. Interactions of PMG and TNFR1 (the receptor of TNF-α) were explored by molecular docking. AAV resuspension was administered before PMG treatment via intravenous injection to overexpress TNF-α in the CCl_4-induced mice. The effects of PMG on liver injury were assessed via CCK-8 assay, AST/ALT level measurement, and HE staining. Cell apoptosis was detected by Hoechst staining, TUNEL staining, and the levels of cleaved caspase-3. mRNA expression of TNF-α and IL-6 was quantified using real-time PCR, while the related proteins were detected by Western blotting. The protein localization of TNF-α was visualized by immunofluorescence assays. PMG effectively protected against hepatotoxicity *in vitro* and *in vivo* by restoring cell survival, decreasing AST, ALT, and reducing apoptosis. TNF-α overexpression counteracted the hepatoprotective effects of PMG, thereby attenuating its regulatory impacts apoptosis and the dysregulation of the PI3K/AKT/NF-κB signaling pathway. Notably, PMG ameliorated hepatotoxicity by restoring the TNF-α-mediated

ARTICLE IN PRESS

signaling pathway, supporting its potential as a novel therapeutic for acute liver injury.

KEY WORDS Acute liver injury; TNF-α; PMG; Hepatoprotection; PI3K/AKT

Abbreviationst PMG, physcion-8-O-β-D-monoglucoside; TNF-α, tumor necrosis factor-α; CCl_4, carbon tetrachloride; AST, Aspartate aminotransferase; ALT, alanine aminotransferase; HE, Hematoxylin and Eosin; PI3K, phosphatidylinositol 3-kinase; AKT, protein kinase B; NF-κB, nuclear factor kappa-B; ICAM-1, intercellular adhesion molecule-1; IL-6, interleukin-6.

ARTICLE IN PRESS

ARTICLE IN PRESS

Introduction

Liver disease is a widespread clinical disease that poses a significant global healthcare challenge. Acute liver injury is the initiating condition of almost all the liver diseases, with persistent liver injury potentially leading to liver cirrhosis and liver cancer[1]. These liver diseases, which have varying etiologies, rapid progression, and serious consequences, will cause liver failure and hepatic encephalopathy if not treated promptly.

Acute liver injury represents an inflammation-mediated process of hepatocellular damage, marked by hepatocyte necrosis and inflammation instigated by immune responses[2]. The immune response mediator, tumor necrosis factor-α (TNF-α), assumes a crucial role in inflammation through its interaction with receptors[3]. TNF-α binding to its receptor, TNFR1, induces hepatocyte apoptosis and inflammatory responses, contributing significantly to the occurrence and progression of acute liver injury[4,5].

Modern pharmacological studies have showed the hepatoprotective effects of Radix et Rhizoma Rhei, a Chinese herb that has been widely used for centuries in treating liver disorders[6,7]. Aloe-Emodin and physcion, the active ingredients of Radix et Rhizoma Rhei, have been reported to exhibit therapeutic effects on acute liver injury, but their poor oral bioavailability limits clinical

ARTICLE IN PRESS

applications[8,9]. Physcion-8-O-β-D-monoglucoside (PMG) represents the glycosides form of physcion (Fig. 1A), demonstrating higher blood concentrations following oral administration compared to aloe-Emodin and physcion[10]. Our SPR analysis confirmed that PMG exhibits reversible binding to TNFR1 with a dissociation constant (Kd) of 376 nM through SPR, while also inhibiting TNF-α-induced cytotoxicity and apoptosis in L929 cells[11]. Whatever, the hepatoprotective effects of PMG in acute liver injury remains unexplored. Our previous study demonstrated that PMG mitigated carbon tetrachloride (CCl_4)-induced acute liver injury in murine models[12].

Given the pivotal role of TNF-α and its receptor TNFR1 in liver injury[4,5], elevated TNF-α levels in acute liver injury can activate the phosphatidylinositol 3-kinase (PI3K)/ protein kinase B (Akt) signaling pathway[13], which initiates and modulates inflammatory responses and apoptotic programs in cell death[14]. This study aims to elucidate the contribution of TNF-α in the protective activities of PMG against acute liver injury. Firstly, the ability of PMG to mitigate TNF-α-induced hepatotoxicity was evaluated *in vitro*. Secondly, we explored the contribution of TNF-α in the protective effects of PMG on CCl_4 injury mice by TNF-α overexpression, and further examined whether PMG mitigates liver injury via the TNF-α-mediated PI3K/AKT/NF-κB

ARTICLE IN PRESS

signaling pathway. Our findings demonstrate that PMG, a novel chemical inhibitor, exhibits a potential candidate drug for acute liver injury treatment.

Materials and methods

Animals and cells

Adult (25 g, 6–8 weeks of age) male ICR mice were acquired from Shanghai SLAC Laboratory Animal Co. Ltd (Production License: SCXK (Shanghai) 2022-0004). All animal studies were carried out in strict accordance with the ARRIVE guidelines. The experimental protocol received ethical approval from the Animal Ethics Committee of Fujian University of Traditional Chinese Medicine (ethics review number: FJTCM IACUC 2021097). All experiments were performed in accordance with the relevant guidelines. The alpha mouse liver 12 (AML-12) cells were obtained from Procell Life Science&Technology Co., Ltd (Wuhan, China) and maintained in DMEM medium supplemented with 10% fetal bovine serum for optimal growth.

Adeno-Associated Virus (AAV) Injections in Mice

For *in vivo* gene transfer, mice were received a single tail vein injection of 100□l AAV resuspension 2 weeks before PMG treatment. AAV2/9-m-TNF (TNF AAV) and AAV2/9-Negative Control (NC AAV) were provided by Hanbio (Shanghai, China) at a titer of 1.1*10^12

ARTICLE IN PRESS

vg/mL and 1.6*10^12 vg/mL respectively. Infection efficiency in the liver was verified by PCR and by Western blot.

Animals and treatments

The mouse model of acute liver injury was generated using intraperitoneal CCl_4 injection (0.1% in corn oil, 0.1mL/10g). PMG (CAS. 26296-54-8) was purchased from Shaanxi Baoji Chenguang Co., Ltd. (Baoji,China). Mice were grouped randomly ($n = 8$ per group): (1) control without any treatment, (2) CCl_4, (3) PMG (20 mg/kg) +CCl_4, PMG was intragastrically administered twice daily for 3 consecutive days before CCl_4 injection. (4) AAV-TNF+PMG +CCl_4, (5) NC-AAV+PMG +CCl_4, (6) 300 mg/kg bifendate (DDB, positive control group). After 16 h CCl_4 treatment, blood was collected via ocular extraction, after which the mice were euthanized by cervical dislocation, and then the liver tissues were harvested.

ARTICLE IN PRESS

Cell administration

Exponentially growing AML-12 cells were harvested and plated in complete medium. After 24 hours of incubation, the culture medium was removed, followed by 4 hours of serum starvation for synchronization. And then cells were pretreated with PMG (80 μM, 40 μM, 20 μM, 10 μM) for 6 hours. TNF-α (20 ng/mL) and actinomycin D (ActD) (10 ng/mL) were added after PMG treatment, and the cells were incubated for another 24 hours.

ARTICLE IN PRESS

Cell viability assay

Following cell treatment, 10 μL of CCK-8 solution was added to each well of a 96-well plate, which was then incubated for 1 h at 37 °C. The absorbance at 450 nm was measured using an Infinite 200PRO microplate reader.

Detection of ALT and AST

Serum samples were collected from animal experiments. Cell culture supernatants were collected from culture well plates at the indicated time points. ALT and AST activity levels were determined in both serum and supernatant using commercially available assay kits, according to the manufacturer's instructions.

HE Staining

Liver tissues were fixed in 4% PFA and embedded in paraffin. The embedded tissues were cut into 4 μm slices. Then, the slices were stained with hematoxylin and eosin (H&E) solution (Solarbio, Nanjing, China) and observed under a light under the light microscope.

Hoechst 33342 Staining

The embedded liver tissues were cut into 4 μm slices. Then the slices were dewaxed in water, rinsed twice with PBS, and stained with Hoechst 33342 staining solution (diluted at 1:100). The number of positive cells were observed and counted under a laser scanning

ARTICLE IN PRESS

confocal microscope.

TUNEL Staining and TNF-α Immunofluorescence Analysis

Embedded tissues were cut into 4-μm sections. Then the slices were dewaxed in water, rinsed twice with PBS, and stained with DAB substrate. TUNEL staining was performed using an apoptosis assay kit (KeyGEN BioTECH, Nanjing, China). After washing with PBS, the sections were then blocked with BSA and incubated with TNF-α primary antibodies diluted at 1:200 (Proteintech, Wuhan, China, cat. No.17590-1-AP) at 4℃ for 24 hours and then stained with fluorophore-conjugated secondary antibodies for 1 hour. The sealed sections were then observed under a Leica fluorescence microscope.

Isolation of total protein and nucleoprotein

The liver tissue was lysed in RIPA lysis buffer for total protein of extraction: total protein in the supernatant was collected after samples were centrifuged. Nucleoprotein were extracted according to the instructions of the nucleoprotein extraction kit (KeyGEN BioTECH, Nanjing, China): The tissue samples was homogenized in Buffer A and then centrifuged. The supernatant was removed, and Buffer C was added. After mixed thoroughly by vortexing, the samples were centrifuged, and the nucleoprotein in supernatant was collected. The concentration of the isolated protein was measured by

ARTICLE IN PRESS

BCA assay.

Western blot analysis

Protein samples were separated by 10% SDS-polyacrylamide gel, and then transferred onto polyvinylirdenediflouride (PVDF) membranes. The blocked membranes were incubated with the indicated primary antibodies: Anti-TNFα (1:1000; cat. No. CPA2174), anti- IL-6 (1:1000; cat. No. CPA4914), anti-AKT (1:1000; cat. No. CPA3481), anti-AKT (pT308) (1:1000; cat. No. CPA1032), anti-PI3K p85 alpha (1:1000; cat. No. CPA3286) and anti- PI3K p85 alpha (pY607) (1:1000; cat. No. CPA7142), anti-PCNA (1:2000; cat. No. CPA9205) and anti-β-actin (1:1000; cat. No. CPA9100) antibodies were obtained from Cohesion Biosciences Limited, and anti-Caspase-3 (1:1000 cat. No.9662), anti- NF-κBp65 (1:1000; cat. No. 8242), anti-IκB (1:1000; cat. No. 4814), anti- pIκB (Ser32) (1:1000; cat. No.2859) were purchased from Cell Signaling Technology, Inc.. Membranes were incubated with the appropriate secondary antibody second antibody on the next day. The bolts were visualized with enhanced chemiluminescence (ECL) staining. Image Lab 4.1 software was used to analyze gray values quantitatively.

Quantitative real-time PCR (qRT-PCR)

RNA samples were obtained from cell or liver tissue sources using Trizol reagent (Vazyme, China). After extraction, the purity of

ARTICLE IN PRESS

the RNA was evaluated. cDNA synthesis was generated with the QRT SuperMix for qPCR (+gDNA wiper) kit following the manufacturer's protocol. Relative mRNA expression levels were determined using the 2-ΔΔCt method, with β-actin as a normalization control. The qRT-PCR was performed using the ChamQ SYBR qPCR Master Mix (Vazyme) and the Applied Biosystems 7900HT real-time PCR system. The primer sequences are shown in Table 1.

Molecular docking of the PMG and TNFR1

To further substantiate the interaction between PMG and TNFR1, we conducted a molecular docking analysis of these two components. Initially, we obtained the 3D protein structure of TNFR1 from the RCSB PDB database. The 2D structure of PMG was generated using ChemBioDraw. Subsequently, molecular docking was conducted with the prepared ligands and proteins utilizing the CDOCKER algorithm within Discovery Studio. Binding affinities of the ligands within the active site were determined using CDOCKER energy scores. Scoring functions, including hydrogen bond counts and distances, CDOCKER energy, and CDOCKER interaction energy, were initially calculated.

Statistical analysis

Data were analyzed statistically using SPSS 20.0 software (Chicago, IL, USA), with results presented as means ± SDs. A

ARTICLE IN PRESS

comparison of the results was performed with one-way ANOVA. Data with normal distribution and homogeneity of variance were compared by LSD test, and the other data were analyzed by Games-Howell test. Correlation analysis was performed using Spearman's rank correlation coefficient. A P value <0.05 was considered statistically significant.

Results

PMG rehabilitates TNF-α-induced injury in AML-12 cells

The AML-12 cell line, derived from normal mouse liver hepatocytes, serves as a valuable model for toxicology research. The *in vitro* model of TNF-α-induced hepatocytes injury model was used to investigate the hepatoprotection efficacy of PMG. Hepatotoxicity of AML-12 induced by TNF-α was sensitized by RNA synthesis inhibitors actinomycin D.

Cell viability, expressed as a percentage relative to control cells, was not significantly affected by the PMG exposure (Fig. 1B). AML-12 cells treated with TNF-α (20 ng/mL) and actinomycin D (10 ng/mL) for 24 hours significantly decreased the cell survival rate compared to the control group, while treatment with 80μM PMG notably increased cell viability after 24 hours (Fig. 1C).

As shown in Fig. 1D, the normal AML-12 cells exhibited

ARTICLE IN PRESS

characteristic hepatocyte morphology, including the presence of peroxisomes and bile canalicular like structure. However, exposure to TNF-α, sensitized by actinomycin D, resulted in the irregular shape, cell shrinkage of AML-12 cells. Notably, PMG effectively reversed these morphological changes, restoring cell shape and structure. PMG at a concentration of 80 □M significantly protected cells against TNF-α-induced cell death.

Aspartate transaminase (ALT) and alanine transaminase (AST) are crucial indicators used to assess liver function and determine liver damage. The model group exhibited significantly elevated ALT and AST levels in culture supernatants compared to the control group. Both 80μM and 40μM PMG treatment significantly reduced ALT and AST levels (Fig. 1E, F), suggesting a protective effect against TNF-α-mediated injury in AML-12 cells.

ARTICLE IN PRESS

Treatment with TNF-α and actinomycin D induced a substantial increase in apoptosis in AML-12 cells, manifested by a marked upregulation of the apoptotic marker cleaved caspase-3. Interestingly, a significant decrease in cleaved caspase-3 levels was observed in AML-12 cells following 24-hour treatment with either 80 μM or 40 μM PMG ($P < 0.05$) (Fig. 1G).

Validation of the PMG–TNFR1 interaction by molecular docking

ARTICLE IN PRESS

Molecular docking was used to assess the binding interaction between PMG and TNFR1. The PDB code (3T6Q) of TNFR1 was acquired from RCSB. The binding energy of the PMG–TNFR1 interaction (CDOCKER ENERGY: 33.3411 kcal/mol) indicated robust binding activities (Fig. 2A-B). The coordination of PMG to TNFR1 was stabilized by hydrogen bonds with residues (Fig. 2C).

TNF-α overexpression abolished the hepatoprotective effects of PMG in CCl_4-induced liver injury in mice

HE staining shows intact hepatic lobule structures and clear central veins in control mice. In contrast, the model group exhibited destruction of the hepatic lobule structure, accompanied by massive hepatocellular necrosis and significant inflammatory cell infiltration. These pathological changes in liver tissue were improved after PMG treatment, and the effect of PMG was reversed by TNF-α overexpression (Fig. 3A)

ALT and AST levels in serum were observed significantly increased in the CCl_4 group when compared to the control group. However, PMG pretreatment significantly reduced these activities. And the effects of PMG on serum AST and ALT were abolished in mice of TNF-α overexpression by AAV-TNF injection (Fig. 3B□C), while there were no changes in the NC-AAV group.

The level of TNF-α and IL-6 in CCl_4 mice liver

ARTICLE IN PRESS

Our results showed significantly elevated protein and mRNA levels of TNF-α and IL-6 in CCl_4-induced liver injury. However, pretreatment with PMG inhibited these increases. Furthermore, TNF-α overexpression was successfully achieved in the TNF-AAV group, in contrast to the NC-AAV group. Interestingly, the inhibitory effect of PMG on TNF-α and IL-6 production was reversed by TNF-α overexpression (Fig. 3D-E).

TNF-α overexpression blocked the inhibition of PMG on CCl_4-caused hepatocyte necrosis

The Hoechst 33342 staining assay were conducted to determine whether TNF-α overexpression inhibited the effects of PMG on cell apoptosis in CCl_4-induced acute liver injury in mice. PMG inhibited CCl_4-induced cell apoptosis and nuclear condensation in liver, while TNF-α overexpression blocked the effect of PMG (Fig. 4A, B).

ARTICLE IN PRESS

The Tunnel staining and TNF-α immunofluorescence analysis revealed a significant increase in both the number of TUNEL-positive cells and TNF-α expression, while PMG pretreatment effectively mitigated these effects. The number of TUNEL-positive cells was significantly positively correlated with TNF-α fluorescence intensity (Pearson=0.935). Furthermore, TNF-α overexpression reversed these protective effects of PMG (Fig. 4C, D).

Additionally, caspase 3 is a critical executioner of apoptosis, the

ARTICLE IN PRESS

cleaved form of caspase 3 serves as a marker for activated caspase-3 was analyzed by Western blot. The level of cleaved caspase-3 expression in the CCl_4 group was significantly higher than the control group. However, treatment with PMG significantly reduced the expression of cleaved Caspase3. Interestingly, TNF-α overexpression blunted these effects (Fig. 4E, F).

TNF-α overexpression blocks the inhibition of PMG on the NF-κB activation through PI3K/ Akt signaling pathway

To elucidate the mechanism by which PMG protects against CCl_4-induced hepatocyte necrosis, the involvement of the PI3K/Akt/NF-κB signaling pathway was investigated. CCl_4 treatment resulted in IκB kinase complex degradation and NF-κB p65 nuclear translocation, thus indicating activation of the NF-κB pathway in the *in vivo* model of acute liver injury. PMG treatment markedly reduced the intranuclear expression of NF-κB p65 (Fig. 5A) and decreased IκB kinase phosphorylation (Fig. 5B, C). In summary, PMG suppressed the nuclear translocation of NF-κ B p65 and activation of the NF-κB pathway.

Furthermore, the roles of PI3K and Akt in the inhibition of PMG on NFκB activation were further investigated. PI3K and Akt phosphorylation increased in CCl_4-induced mice. However, PMG inhibited not only NF-κB activation but also PI3K/Akt

ARTICLE IN PRESS

phosphorylation. Intriguingly, TNF-α overexpression abrogated the modulation of PMG on PI3K/Akt/NFκB signaling pathway resulting in increased PI3K and Akt phosphorylation (Fig. 5B, D, E), as well as the activation of NFκB. Collectively, these data strongly support the conclusion that PMG inhibits TNF-α-induced hepatocyte necrosis via a mechanism dependent on the PI3K/Akt/NF-κB pathway.

Discussion

The inflammatory response is a key driver in liver injury progression. TNF-α, a multifaceted cytokine primarily produced by activated monocytes and macrophages, and extensively involved in this process, influencing immune system development, cell growth, and hepatocyte death[15]. The TNF receptors are abundant in liver, makes the hepatocytes highly sensitive to TNF-α. TNF-α initiates diverse biological effects through signaling pathways activated TNFR1[16].

The application of Radix et Rhizoma Rhei in the treatment of hepatic disorders dates back several centuries in traditional Chinese medicine. PMG, a compound found in the extract of *Rheum officinale* (one of the origins of TCM Rhizoma Rhei). DDB, a synthetic schisandrin C analog and clinically used hepatoprotective agent from Schisandra chinensis, serves as a positive control in hepatoprotective research[17, 18]. Our molecular docking analysis

ARTICLE IN PRESS

revealed that PMG exhibited favorable binding affinity toward TNFR1, with a CDOCKER interaction energy of -33.3411 kcal/mol. To further investigate the protective effects of PMG against TNF-α-induced liver injury, *in vitro* experiments were conducted to assess its hepatoprotective activity. Our results demonstrated that the PMG protects AML-12 cells from TNF-α-induced hepatotoxicity, as evidenced by high cell viability, low AST and ALT level in supernatants. And markedly downregulated the expression of the apoptosis effector protein cleaved caspase 3. These suggest that PMG exerts significant protective effects against TNF-α-induced hepatocyte injury, which may be attributed to its anti-apoptotic activity through inhibition of caspase-mediated pathways.

To further validate the role of TNF in the potential mechanisms of PMG, we conducted in vivo experiments with TNF-α overexpression. CCl_4-induced liver injury in rodents serves as a well-established model for in vivo study. With the liver as the primary site for plasmid DNA uptake[19], tail vein injection of TNF-α overexpression virus selectively targets the liver. The hepatoprotective efficacy of PMG was demonstrated by its ability to attenuate CCl_4-induced pathological changes, including necrosis, and reduce serum AST and ALT activities. However, these regulatory effects of PMG were abolished by hepatic overexpression of TNF-α.

ARTICLE IN PRESS

TNF-α-mediated apoptosis in liver injury was assessed using Hoechst 33342 and TUNEL staining (with TNF-α fluorescence). The results revealed that PMG significantly reduced CCl_4-induced hepatocyte apoptotic cells and TNF-α fluorescence intensity, accompanied with the downregulation of cleaved caspase-3 expression. Notably, the number of TUNEL-positive cells was significantly positively correlated with TNF-α fluorescence intensity (Pearson=0.935). The effects of PMG on apoptosis and TNF-α were reversed by TNF-α overexpression. These findings suggest that PMG exerts its anti-apoptotic effects in liver injury through a mechanism involving TNF-α signaling.

The regulatory effect of NF-κB signaling and anti-apoptotic pathway on TNF-α was observed in acute liver injured model induced by CCl_4[20, 21]. TNF-α-induced cell death requires the canonical NF-κB signaling pathway[4]. The PI3K/AKT signaling pathway plays a crucial role in mediating TNF-α-induced inflammatory responses and cellular damage[22-24]. PI3K is activated upon interaction with growth factor receptors or phosphorylated connexins, undergoing a conformational change. The resulting production of PIP3 recruits and activates Akt at the plasma membrane. Then, as a downstream target of AKT, the NF-κB also shows increased activation.

This pathway centers on NF-κB, a nuclear transcription factor

ARTICLE IN PRESS

regulating genes crucial for apoptosis and inflammation. In its inactive form, cytoplasmic NF-κB is normally inhibited by IκB proteins. TNF-α, a key activator, binds to its receptor TNFR1, recruiting TRADD, which then recruits TRAF2 and NIK. NIK/MEKK1-mediated phosphorylation of IKK1 and IKK2 subsequently leads to IκB phosphorylation. Phosphorylation of IκB by the IKK complex (IKK1/IKKa, IKK2/IKKb, and IKK3/IKKg) triggers IκB ubiquitination and degradation, releasing NF-κB dimers to translocate to the nucleus, bind DNA, and activate target genes[25]. This transcriptional activation mechanism triggers expression of pro-inflammatory mediators such as TNF-α and IL-6[26], which promote inflammatory cell infiltration and exacerbate inflammatory responses. Additionally, it upregulates caspase genes to activate caspase-dependent apoptosis pathways[27]. Caspases are key enzymes in apoptosis, with caspase-3 being the most critical executioner protease in the caspase cascade. Once activated, it cleaves (the cleaved caspase-3) targets like DNA-PK to trigger cell death[28].

Our work demonstrated that overexpression of TNF-α blocked the inhibition of PMG on the NF-κB activation, by altering several key downstream events, including caspase-3 activation, PI3K and Akt phosphorylation, and NF-κB nuclear translocation, implying that induction of TNF-α was involved in the PMG regulation of PI3K/AKT/

ARTICLE IN PRESS

NF-κB pathway. Therefore, our data revealed that TNF-α/PI3K/Akt/NF-κB axis was the main mechanism of PMG alleviates acute liver injury (Fig. 6). These data provide novel evidence on TNF-α function in the therapeutic effect of PMG in acute liver injury.

Although the PI3K/AKT pathway is implicated the protect effects of PMG in TNF-α-mediated liver injury, the potential involvement of alternative signaling pathways warrants further investigation in subsequent studies to fully elucidate the molecular mechanisms.

5. Conclusions

In summary, PMG exerts a hepatoprotective effect against TNF-α-induced acute liver injury, primarily by suppressing TNF-α/PI3K/Akt/NF-κB signaling. These findings support the development of PMG as a novel therapeutic agent for acute liver injury.

ARTICLE IN PRESS

Data availability

Data are available from the corresponding author on reasonable request.

Funding

This work was supported by the National Natural Science Foundation of China under Grant (NO. 82204378); and the School Fund of Fujian University of Traditional Chinese Medicine under Grant (NO. X2019007-Tanlent; NO. XJC2022003).

ARTICLE IN PRESS

Declaration of interests

The authors have no conflicts of interest to declare.

ARTICLE IN PRESS

ARTICLE IN PRESS

References

1. Schümann, J. & Kammüller, M. in *Encyclopedia of Immunotoxicology* (ed Hans-Werner Vohr) 1-6 (Springer Berlin Heidelberg, 2005).
2. Shojaie, L., Iorga, A. & Dara, L. Cell Death in Liver Diseases: A Review. *International journal of molecular sciences* **21**, doi:10.3390/ijms21249682 (2020).
3. Chen, G. & Goeddel, D. V. TNF-R1 signaling: a beautiful pathway. *Science* **296**, 1634-1635, doi:10.1126/science.1071924 (2002).
4. Cubero, F. J. *et al.* TNFR1 determines progression of chronic liver injury in the IKKgamma/Nemo genetic model. *Cell Death Differ.* **20**, 1580-1592, doi:10.1038/cdd.2013.112 (2013).
5. Ding, W. X. & Yin, X. M. Dissection of the multiple mechanisms of TNF-alpha-induced apoptosis in liver injury. *J. Cell. Mol. Med.* **8**, 445-454, doi:10.1111/j.1582-4934.2004.tb00469.x (2004).
6. Zhuang, T. *et al.* Hepatoprotection and hepatotoxicity of Chinese herb Rhubarb (Dahuang): How to properly control the "General (Jiang Jun)" in Chinese medical herb. *Biomed. Pharmacother.* **127**, 110224, doi:10.1016/j.biopha.2020.110224 (2020).
7. Wang, J. B. *et al.* Hepatotoxicity or hepatoprotection? Pattern recognition for the paradoxical effect of the Chinese herb Rheum palmatum L. in treating rat liver injury. *PLoS One* **6**, e24498, doi:10.1371/journal.pone.0024498 (2011).
8. Arosio, B. *et al.* Aloe-Emodin quinone pretreatment reduces acute liver injury induced by carbon tetrachloride. *Pharmacol. Toxicol.* **87**, 229-233, doi:10.1034/j.1600-0773.2000.d01-79.x (2000).
9. Zhang, L. Y., Su, W. H., Xiong, Y. & Wang, D. Protective effect of physcione on acute liver injury in rats. *Chinese Journal of Primary Medicine and Pharmacy* **14**, 2014-2015 (2007).
10. Cheng, W. H. *Study on the pharmacokinetics of Polygonum multiflorum Thunb.* , Beijing University of Chinese Medicine, (2020).
11. Cao, Y. *et al.* Identification of a ligand for tumor necrosis factor receptor from Chinese herbs by combination of surface plasmon resonance biosensor and UPLC-MS. *Anal. Bioanal. Chem.* **408**, 5359-5367, doi:10.1007/s00216-016-9633-6 (2016).
12. Chen, T., Chen, Y. P., Cao, Y. J. & Nan, L. H. The effects of Physcion-8-O-β-D-monoglucoside on acute liver injury induced by CCl4 in mice. *Fujian Journal of Traditional Chinese Medicine* **53**, 18-21+27, doi:10.13260/j.cnki.jfjtcm.012419 (2022).
13. Gao, Z. *et al.* Hydroxytyrosol Alleviates Acute Liver Injury by Inhibiting the TNF-α/PI3K/AKT Signaling Pathway via Targeting TNF-α Signaling. *Int J Mol Sci.* **25**,12844, doi: 10.3390/ijms252312844 (2024).

ARTICLE IN PRESS

14. Liu, Y. & Tie, L. Apolipoprotein M and sphingosine-1-phosphate complex alleviates TNF-alpha-induced endothelial cell injury and inflammation through PI3K/AKT signaling pathway. *BMC Cardiovasc. Disord.* **19**, 279, doi:10.1186/s12872-019-1263-4 (2019).
15. Cai, L. *et al.* AMPK dependent protective effects of metformin on tumor necrosis factor-induced apoptotic liver injury. *Biochem. Biophys. Res. Commun.* **465**, 381-386, doi:10.1016/j.bbrc.2015.08.009 (2015).
16. Schwabe, R. F. & Brenner, D. A. Mechanisms of Liver Injury. I. TNF-alpha-induced liver injury: role of IKK, JNK, and ROS pathways. *Am. J. Physiol. Gastrointest. Liver Physiol.* **290**, G583-589, doi:10.1152/ajpgi.00422.2005 (2006).
17. Yuan, W., Jian, F., &Rong, Y. Bifendate inhibits autophagy at multiple steps and attenuates oleic acid-induced lipid accumulation. *Biochem. Biophys. Res. Commun.* **631**, 115-123, doi:10.1016/j.bbrc.2022.09.067, (2022).
18. Zou, J., Qi, F., Ye, L., &Yao, S. Protective role of grape seed proanthocyanidins against ccl4 induced acute liver injury in mice. *Med. Sci. Monit.* **22**, 880-889, doi:10.12659/MSM.895552, (2016).
19. Chen, X. & Calvisi, D. F. Hydrodynamic transfection for generation of novel mouse models for liver cancer research. *Am. J. Pathol.* **184**, 912-923, doi:10.1016/j.ajpath.2013.12.002 (2014).
20. Dong, Y. *et al.* The protective or damaging effect of Tumor necrosis factor-alpha in acute liver injury is concentration-dependent. *Cell & bioscience* **6**, 8, doi:10.1186/s13578-016-0074-x (2016).
21. Li, J. *et al.* Hepatoprotective Effects of Heracleum candicans Against Carbon Tetrachloride-Induced Acute Liver Injury in Rats. *Dose Response* **19**, 15593258211029510, doi:10.1177/15593258211029510 (2021).
22. Chen, H. W., Lin, A. H., Chu, H. C., Li, C. C. & Liu, K. L. Inhibition of TNF-α-Induced Inflammation by andrographolide via down-regulation of the PI3K/Akt signaling pathway. *J. Nat. Prod.* **74**, 2408-2413 (2011).
23. Kettritz, R. *et al.* Phosphatidylinositol 3-kinase controls antineutrophil cytoplasmic antibodies-induced respiratory burst in human neutrophils. *J. Am. Soc. Nephrol.* **13**, 1740-1749, doi:10.1097/01.asn.0000019411.36000.06 (2002).
24. Li, W. S. *et al.* Naringin inhibits TNF-α induced oxidative stress and inflammatory response in HUVECs via Nox4/NF-κ B and PI3K/Akt pathways. *Curr Pharm Biotechnol.* **59**, 868-879, doi:10.2174/1389201015666141111114442 (2014).
25. Bottero, V., Withoff, S. & Verma, I. M. NF-kappaB and the

ARTICLE IN PRESS

regulation of hematopoiesis. *Cell Death Differ.* **13**, 785-797, doi:10.1038/sj.cdd.4401888 (2006).
26. Jeoung, B. R. *et al.* Ganghwaljetongyeum, an anti-arthritic remedy, attenuates synoviocyte proliferation and reduces the production of proinflammatory mediators in macrophages: the therapeutic effect of GHJTY on rheumatoid arthritis. *BMC Complement. Altern. Med.* **13**, 47, doi:10.1186/1472-6882-13-47 (2013).
27. Maelfait, J., Liverpool, L. & Rehwinkel, J. Nucleic Acid Sensors and Programmed Cell Death. *J. Mol. Biol.* **432**, 552-568, doi:10.1016/j.jmb.2019.11.016 (2020).
28. Cheng, C. Y. *et al.* Ferulic acid inhibits nitric oxide-induced apoptosis by enhancing GABA(B1) receptor expression in transient focal cerebral ischemia in rats. *Acta Pharmacol. Sin.* **31**, 889-899, doi:10.1038/aps.2010.66 (2010).

ARTICLE IN PRESS

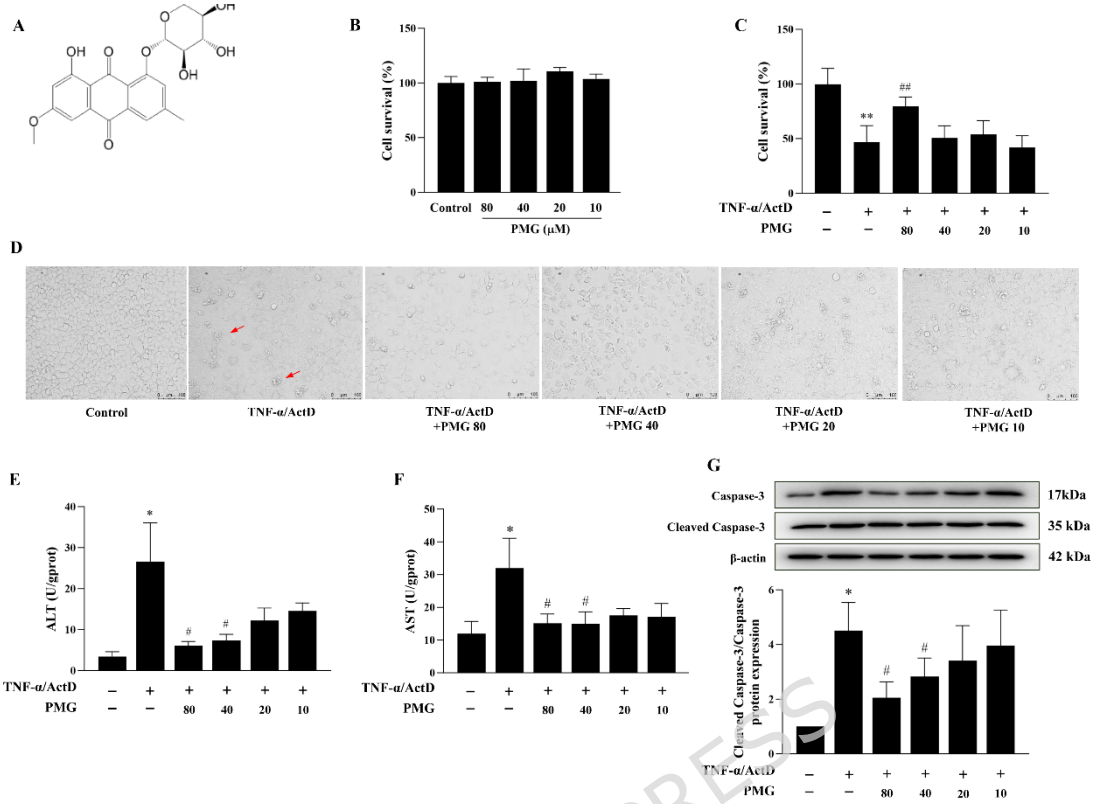

Fig. 1 PMG attenuated TNF-α-induced injury in AML-12 cells.

A. The chemical structure of PMG. B. Effect of PMG (10-80 μM) on AML-12 cell viability (n=6). C. The inhibitory effect of PMG on TNF-α-mediated cell cytotoxicity (n=6). D. Brightfield microscopy (200× magnification) of TNF-α-induced AML-12 cells pretreated with PMG (10-80 μM) for 24 h. E-F. Effects of PMG on AST and ALT levels in the culture supernatant (n=6). G. Western blot analysis of the cleaved caspase-3 in AML-12 cells (n=3). All data are presented as the means ± SDs. $^{**}P$＜0.01, $^{*}P$＜0.05 vs the Control group; $^{\#\#}P$＜0.01, $^{\#}P$＜0.05 vs the TNF-α/ActD group.

ARTICLE IN PRESS

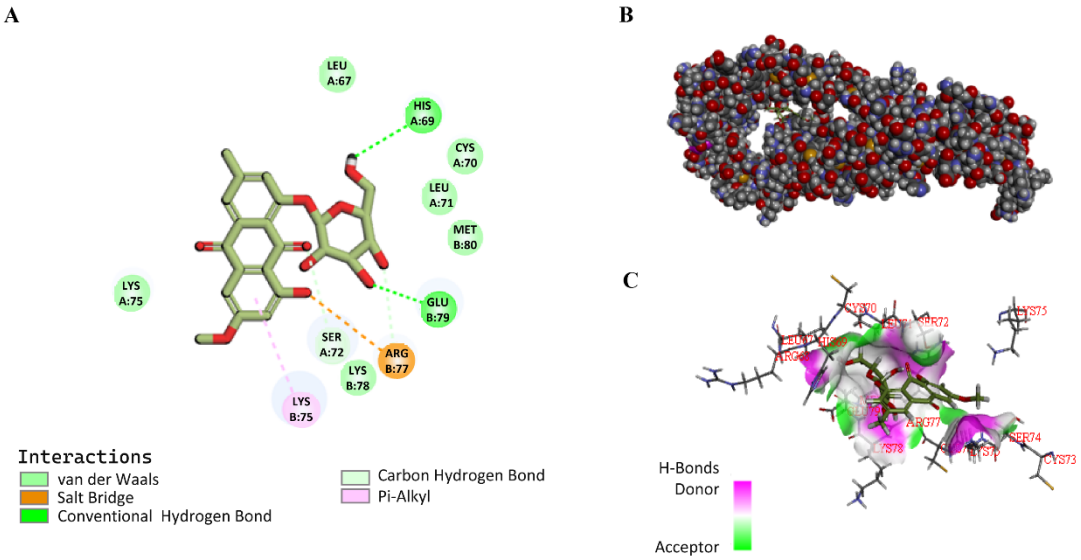

Fig. 2 Molecular docking analysis of PMG and TNFR1.

A. 2D interaction diagram of PMG in the active site of TNFR1. B. The PMG-TNFR1 complex. C. Hydrogen bond interaction diagram of PMG and TNFR1.

ARTICLE IN PRESS

ARTICLE IN PRESS

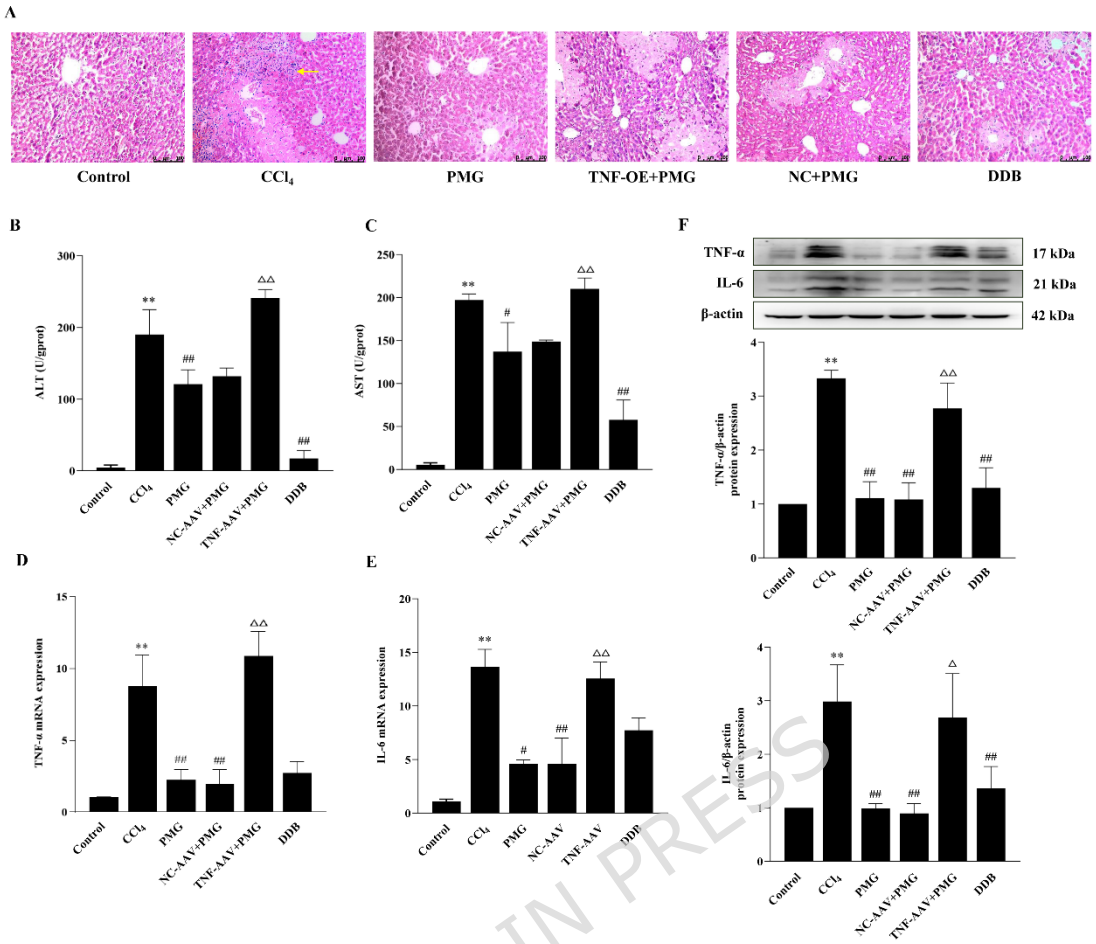

Fig. 3 TNF-α overexpression abolished the hepatoprotective effects of PMG in CCl_4 mice

A. Pathological lesion staining of mouse liver (HE, ×200). The yellow arrow indicates the inflammatory cell infiltration. B-C. Serum levels of aspartate transaminase (ALT) and alanine transaminase (AST) in CCl_4 mice (n = 8). D-E. RT-qPCR measurements of TNF-α and IL-6 in mice treated with CCl_4 with or without AVV-TNF compared to untreated controls (n = 6). F. Western blot analysis of TNF-α and IL-6 in each treatment group (n = 6). All data are expressed as the means ± SDs. $^{**}P$ 0.01 vs the Control group; $^{\#\#}P$ 0.01, $^{\#}P$ 0.05 vs the CCl_4 group; $^{\triangle\triangle}P$ 0.01, $^{\triangle}P$ 0.05 vs the PMG

ARTICLE IN PRESS

group.

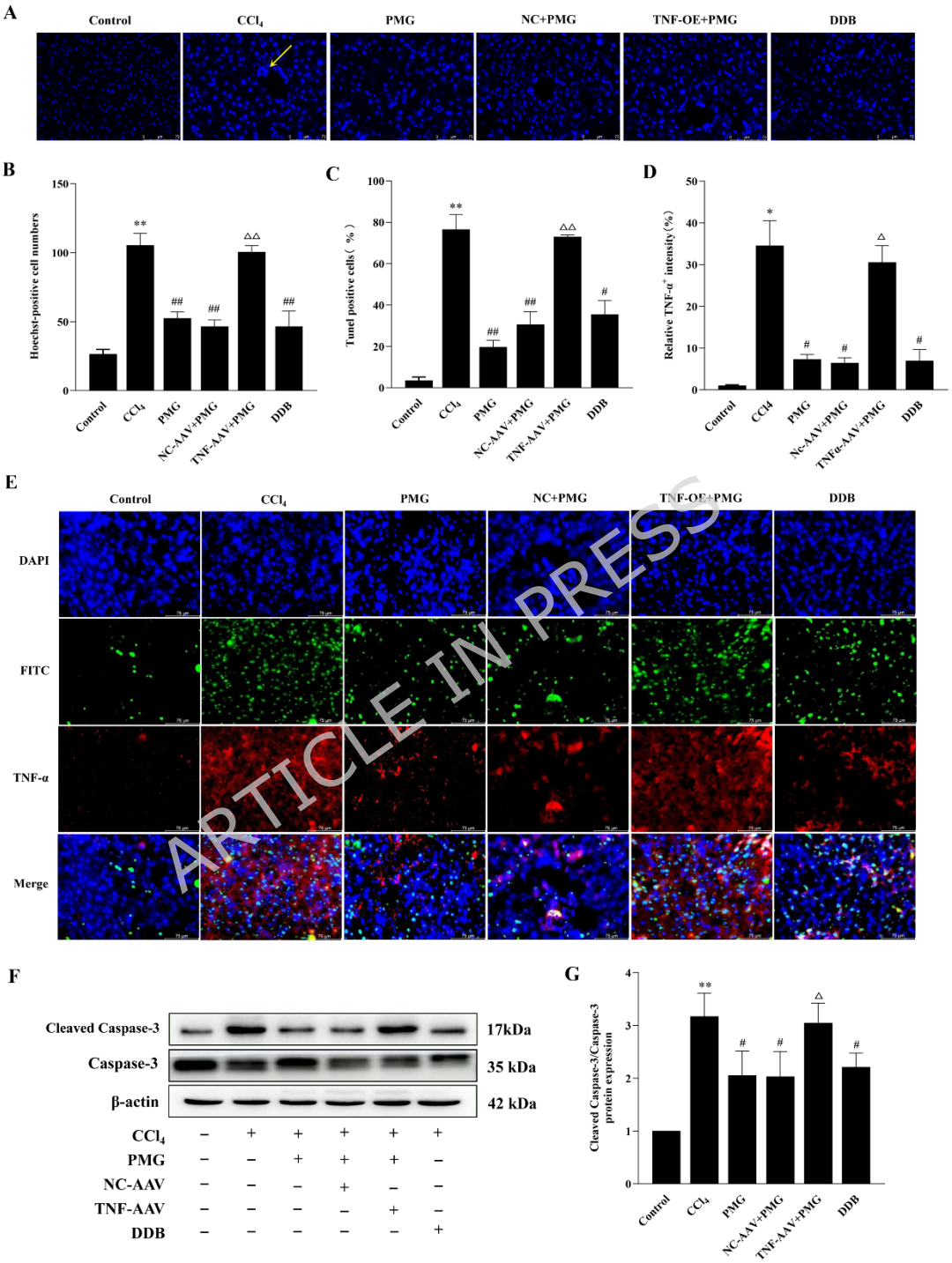

Fig. 4 TNF-α overexpression blocked the inhibition of PMG on CCl_4-caused hepatocyte necroptosis.

A. The Hoechst 33342 staining images of cell apoptosis (×400).

ARTICLE IN PRESS

The yellow arrow indicates the apoptotic cells were dyed blue. B. Statistical analysis of Hoechst 33342 staining (n = 6). C-E. TUNEL staining and TNF-α immunofluorescence analysis under the same field of view (×400). TUNEL-positive cells were identified with green fluorescence, TNF-α labeled by red fluorescence, and DAPI stained with in blue. Statistical analysis of TUNEL staining (C) and TNF-α immunofluorescence intensity(D) (n = 3). F-G. Western blot analysis of the cleaved caspase-3 in liver tissues of mice in each group (n = 5). All data are expressed as the means ± SDs $^{**}P$<0.01 vs the Control group; $^{\#\#}P$<0.01, $^{\#}P$<0.05 vs the CCl_4 group; $^{\triangle}P$<0.05 vs the PMG group.

ARTICLE IN PRESS

ARTICLE IN PRESS

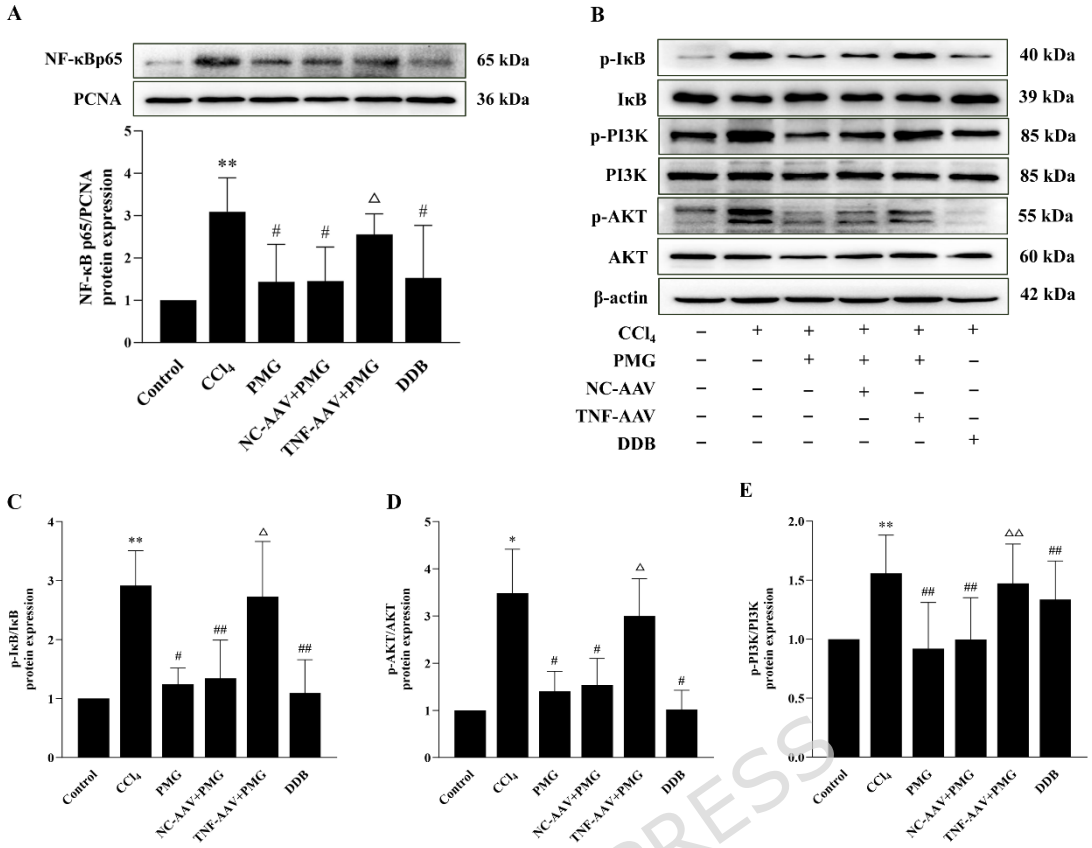

Fig. 5 TNF-α overexpression reversed the regulation of PMG on PI3K/AKT/NF-κB signaling protein expression in CCl_4 mice.

A. Expressions of NF-κB p65 proteins in nucleus. The internal standard for nucleoprotein was proliferating cell nuclear antigen (PCNA). B-E. The phosphorylation levels of IκB, PI3K and AKT in liver tissues were detected by western blotting analysis. All data are expressed as the means ± SDs (n = 5-6). $^{*}P$ 0.05, $^{**}P$ 0.01vs the Control group; $^{\#}P$ 0.05, $^{\#\#}P$ 0.01vs the CCl_4 group; $^{\triangle}P$ 0.05, $^{\triangle\triangle}P$ 0.01 vs the PMG group.

ARTICLE IN PRESS

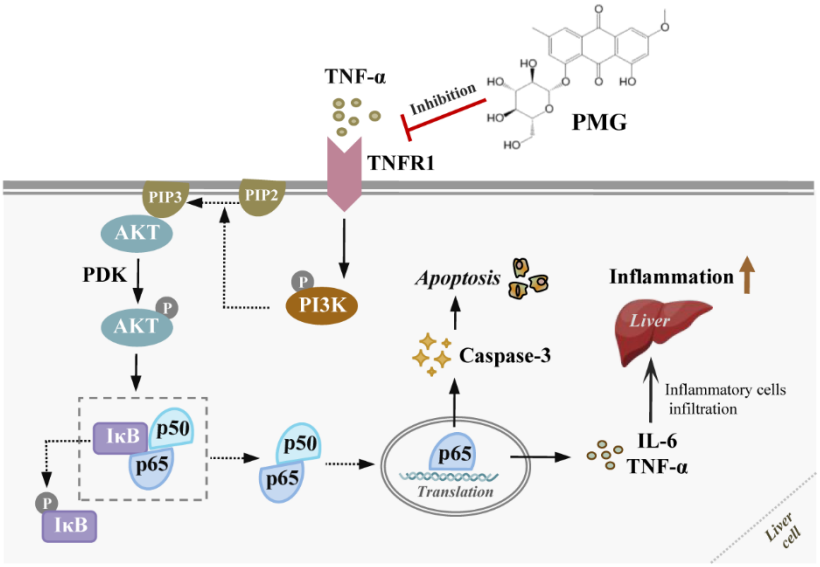

Fig. 6 The underlying mechanisms by which PMG attenuates hepatotoxicity by inhibiting TNF-α injury.

Schematic diagram illustrating the involvement of the TNF-α/PI3K/Akt/NF-κB signaling pathway in the effects of PMG on CCl_4-induced acute liver injury.

ARTICLE IN PRESS

ARTICLE IN PRESS

A

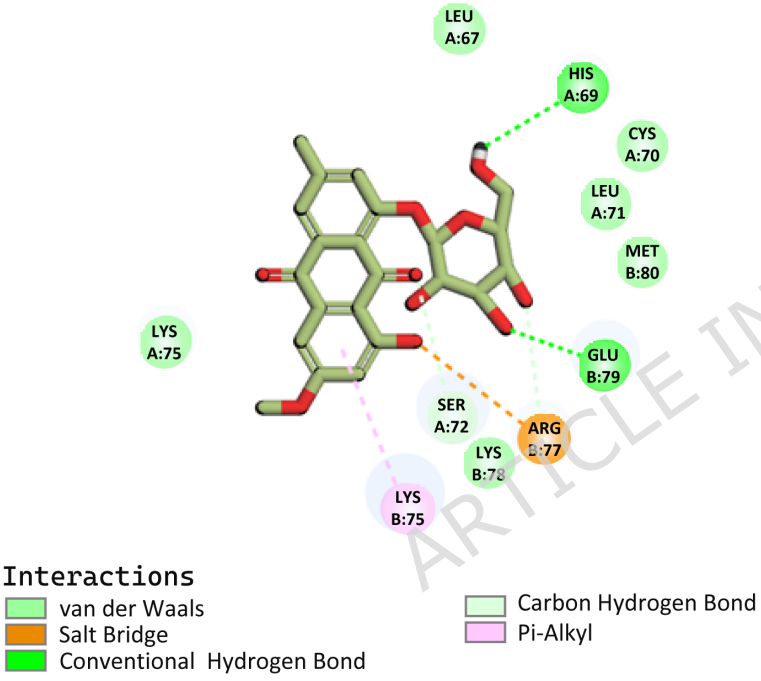

B

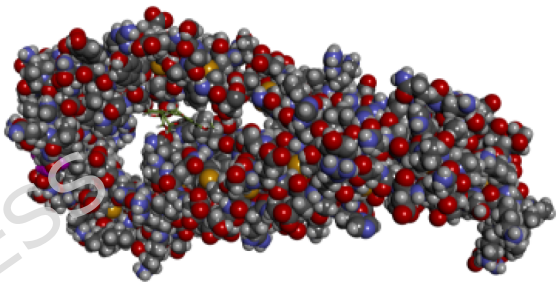

C

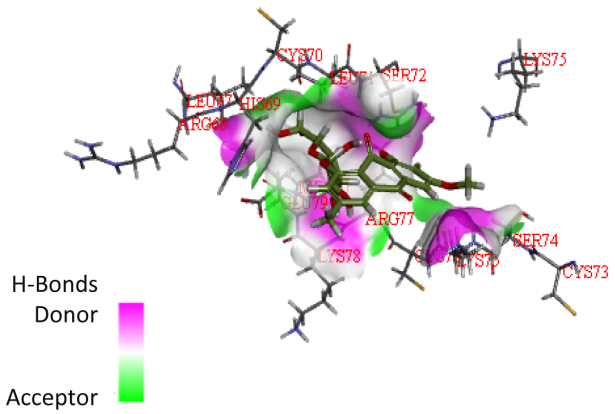

ARTICLE IN PRESS

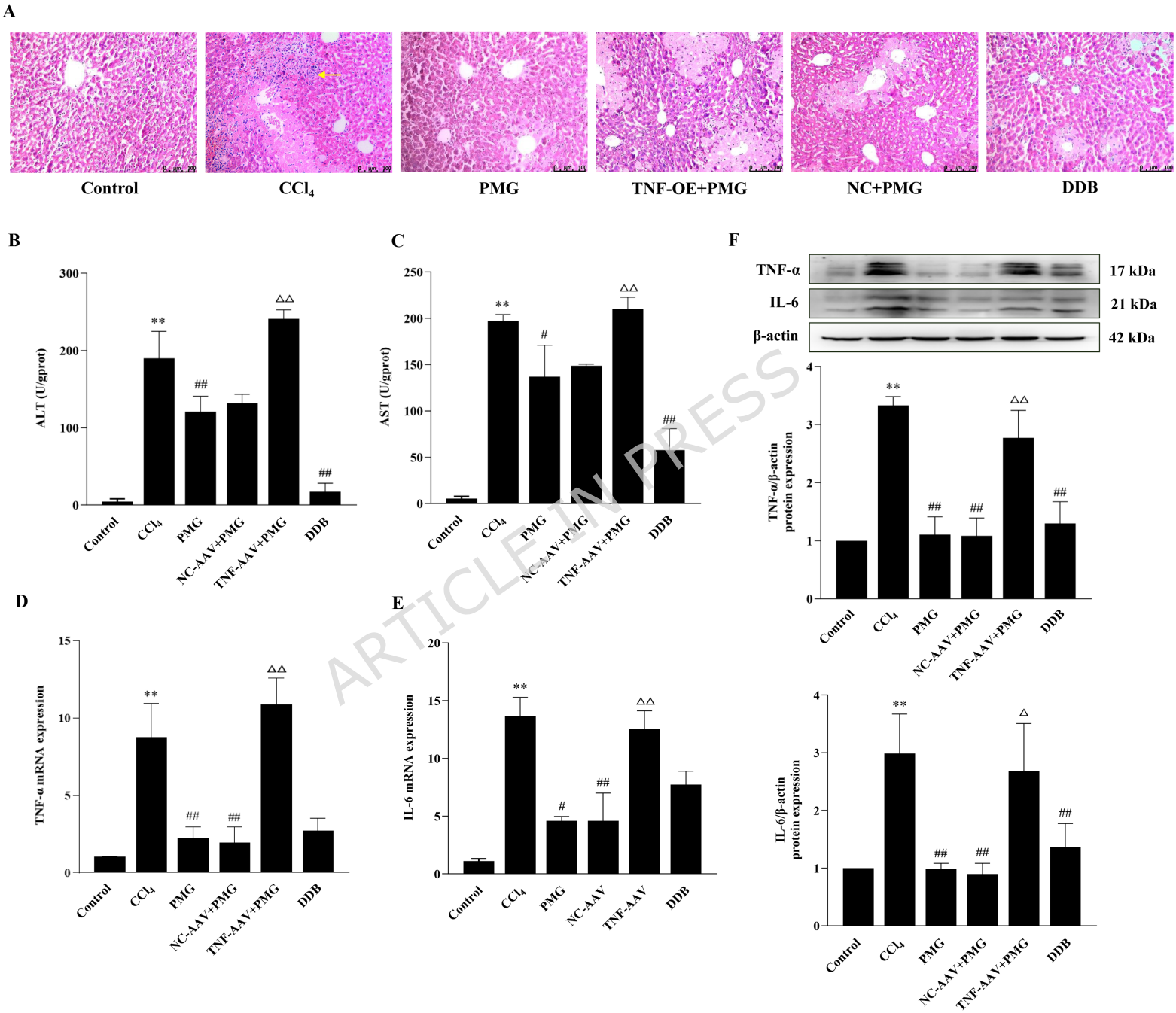

ARTICLE IN PRESS

ARTICLE IN PRESS

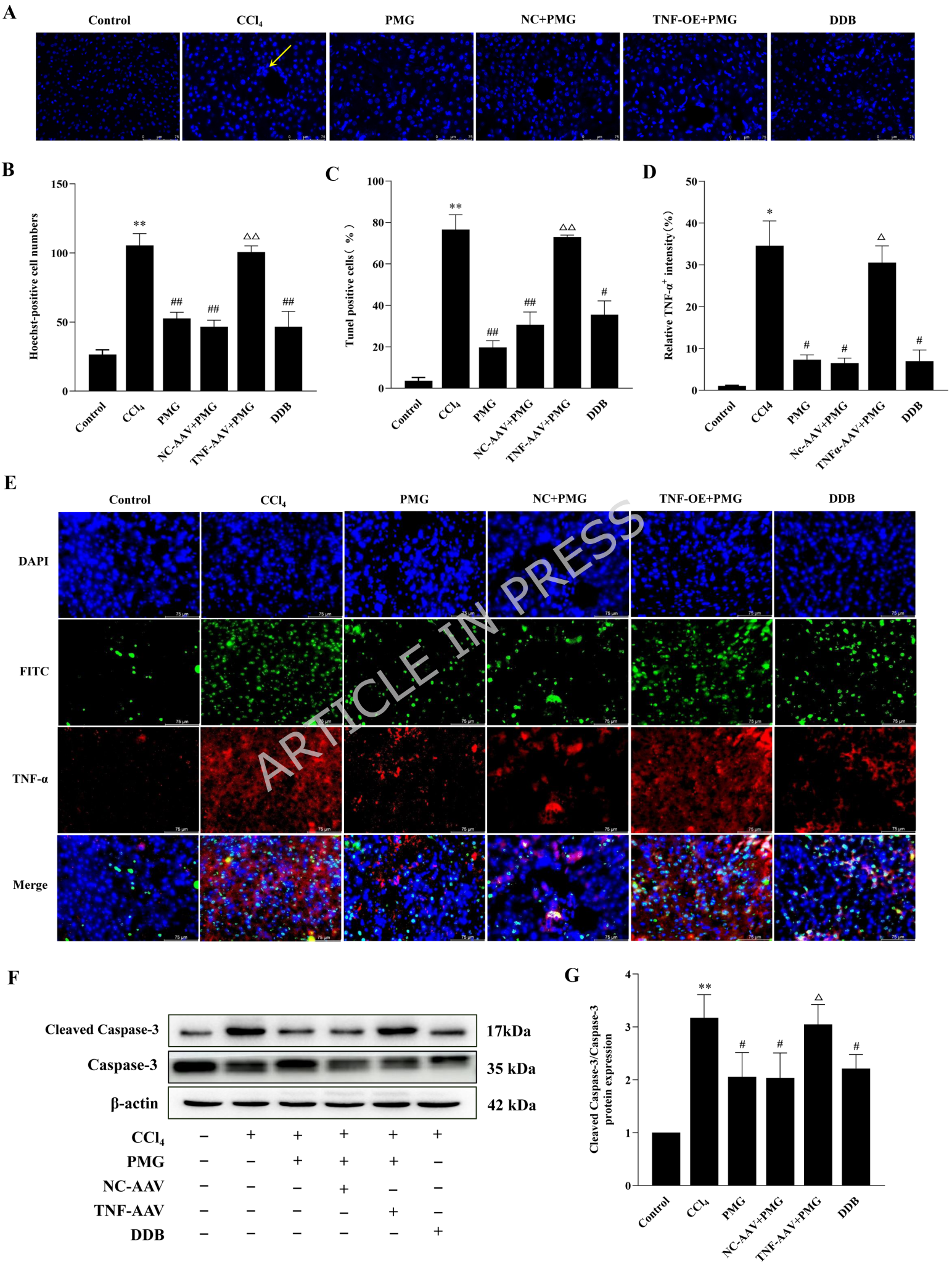

ARTICLE IN PRESS

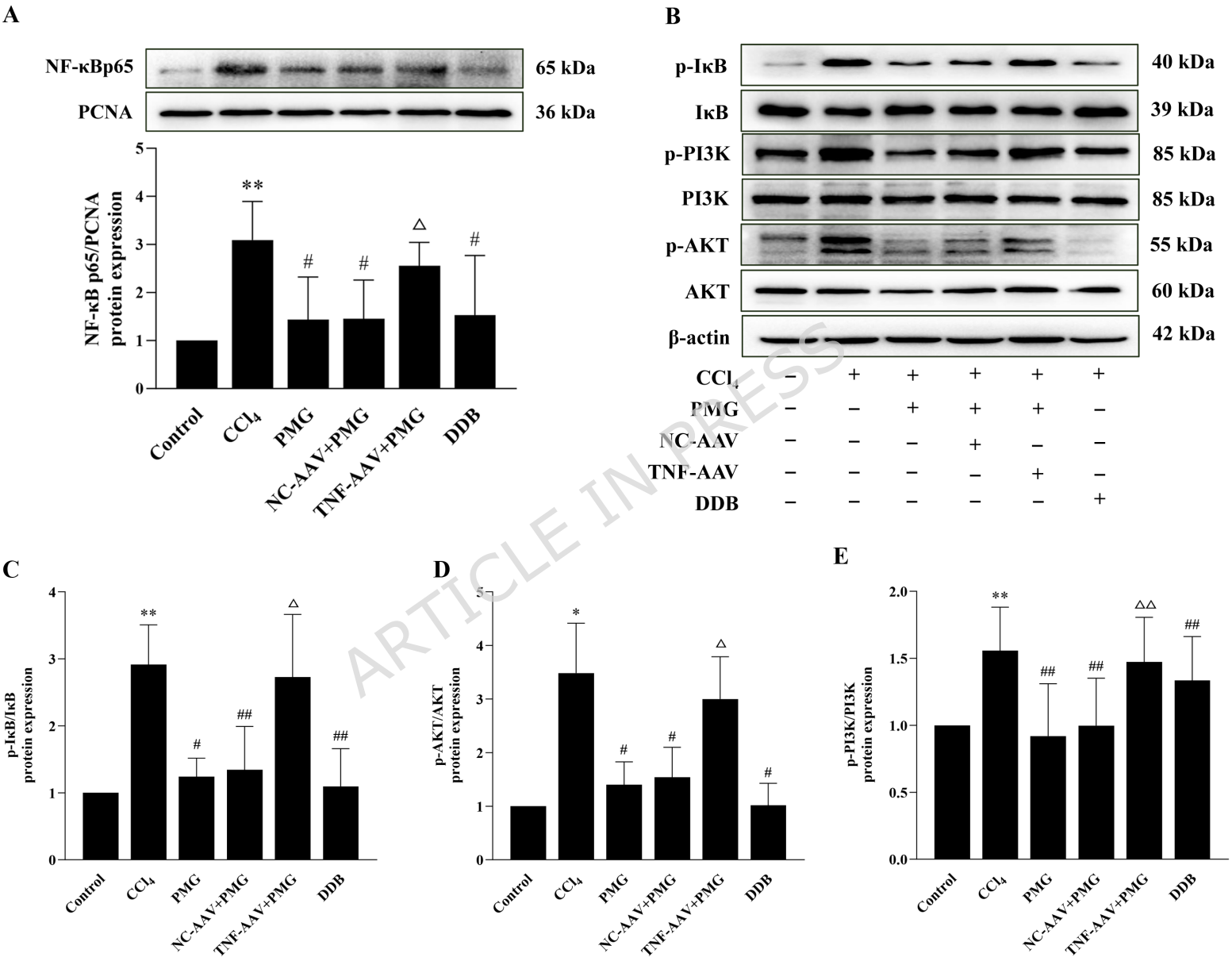

ARTICLE IN PRESS

ARTICLE IN PRESS

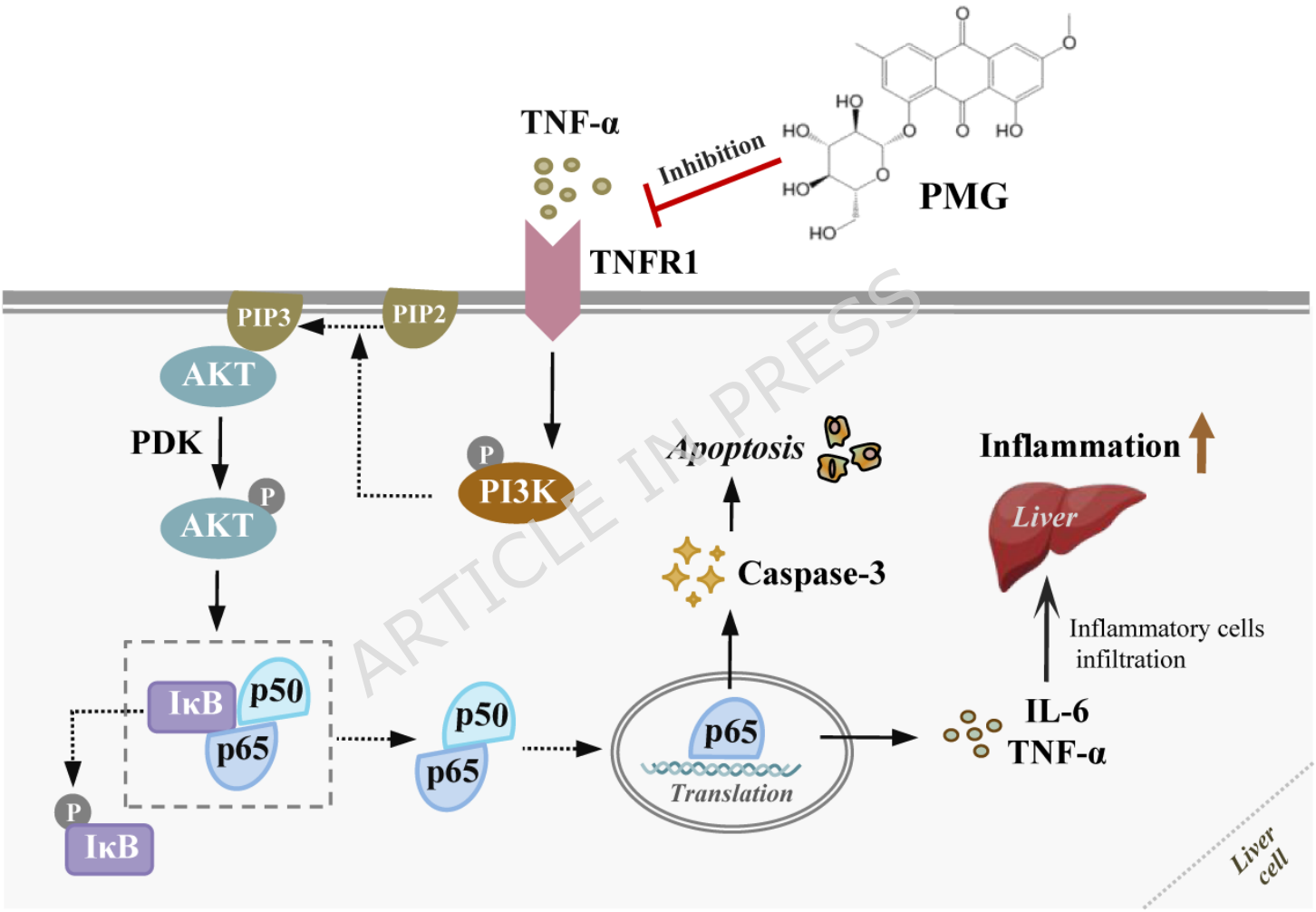

ARTICLE IN PRESS

ARTICLE IN PRESS

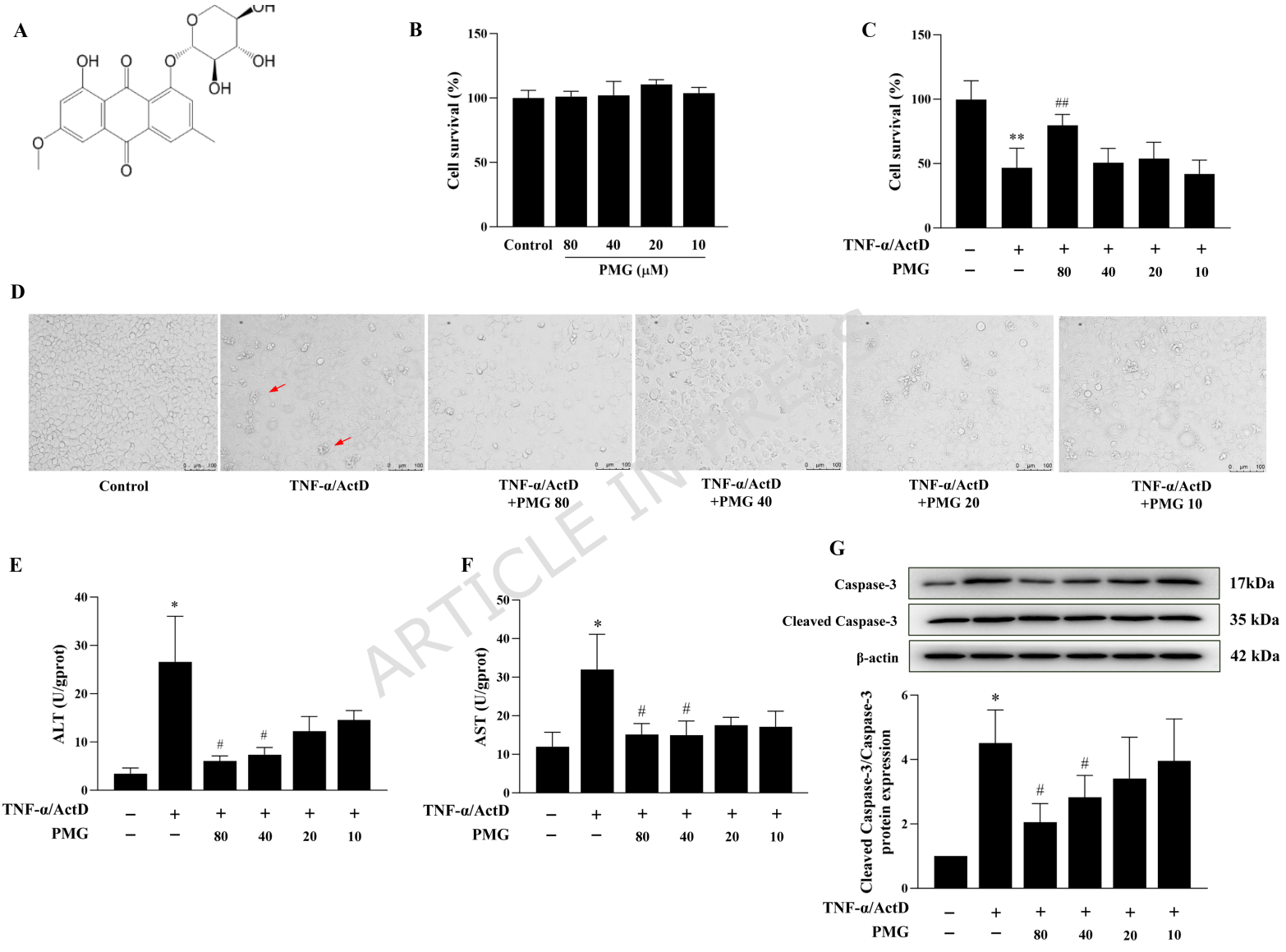

ARTICLE IN PRESS

Table 1. The sequences of the primers used in quantitative real-time PCR (qRT-PCR).

Gene	Forward (3’-5’)	Reverse (5’-3’)
GAPDH	ATCTTCTTGTGCAGTGCCAGCCTC	TTTGCCACTGCAAATGGCAGCC
TNF-α	TCATGCACCACCATCAAGGA	GACATTCGAGGCTCCAGTGAA
IL-6	AACCACGGCCTTCCCTACTT	TTGGGAGTGGTATCCTCTGTGA

ARTICLE IN PRESS